JCTC Journal of Chemical Theory and Computation

Letter

pubs.acs.org/JCTC

Optical Signature of Formation of Protein Corona in the Firefly Luciferase-CdSe Quantum Dot Complex

Jennifer M. Elward,[#] Flaviyan Jerome Irudayanathan,[‡] Shikha Nangia,*[,§] and Arindam Chakraborty*[,†]

[#]Army Research Laboratory, Aberdeen Proving Ground, Aberdeen, Maryland 21005, United States

[†]Department of Chemistry, [‡]Department of Biomedical and Chemical Engineering, and [§]Syracuse Biomaterials Institute, Syracuse University, Syracuse, New York 13244, United States

Supporting Information

ABSTRACT: Theoretical investigation of protein corona is challenging because of the size of the protein-dot complex. In this work, we have addressed this computational bottleneck by combining pseudopotential + explicitly correlated Hartree−Fock QM calculations with molecular mechanics, molecular dynamics, and Monte Carlo techniques. The optical gap of a 5 nm CdSe quantum dot ($Cd_{1159}Se_{1183}$) was computed by sequential addition of luciferase (Lu), and a red shift of 8 nm in the λ_{max} of protein corona ($CdSe-Lu_7$) was observed.

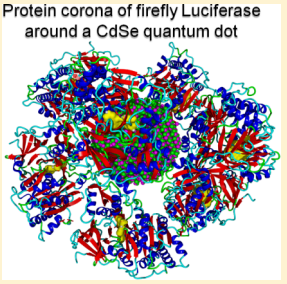

When quantum dots (QDs) are exposed to biological media, their surfaces adsorb biomolecules, generally proteins, present in the system.[1] Formation of protein corona on the surface of quantum dots directly influences their physical, chemical, and biochemical properties. In this work, we present theoretical investigation of the interaction of a 5 nm CdSe ($Cd_{1159}Se_{1183}$) quantum dot with firefly luciferase enzyme by analyzing the change in the optical property of the quantum dot due to corona formation. The objective of this work is to correlate the spectral shift of the QD with structure and stoichiometry of the protein corona.

Quantum dots are being used as nanoprobes for biological systems because of their nanoscale dimensions and sensitivity of their optical properties to local chemical environment. For example, CdSe quantum dots have been used for determination of local pH in cells[2−6] and for detection of various biomolecules such as DNA[7] and glucose.[8] They have also been used for bioimaging[9] including *in vivo* imaging of tumor cells.[10] Quantum dots functionalized with bioluminescent proteins such as luciferase have been used for mapping of lymph nodes,[11] detection of nucleic acids,[12] *in vivo* imaging,[13,14] photodynamic therapy,[15] and investigation of bioluminescence resonance energy transfer (BRET).[16−20] However, there is a growing body of evidence that shows that it is the QD-protein complex and not the pristine quantum dot that is important for biological activity.[21−26]

The computational treatment of the QD-protein complex is challenging because of the size of the system. This problem is further aggravated for calculation of optical properties because it requires quantum mechanical description of both the ground and excited electronic states. For small CdSe quantum dots with 1.3 nm diameter, Anandampillai et al.[27] have investigated the effect of QD-DNA interactions using density functional theory (DFT). Kim et al. have also studied the effect of bioconjugation on a CdSe-Adenine complex utilizing DFT methodology.[28] Ligated quantum dot systems have been studied extensively using the DFT based approach.[29−33] However, an all-electron DFT calculation is computationally prohibitive for the present system. Our system consists of a 5 nm CdSe quantum dot ($Cd_{1159}Se_{1183}$) with 2342 heavy atoms. Each luciferase enzyme molecule contributes 8423 heavy atoms. The protein corona on the surface was found to consist of seven enzyme molecules making the total number of heavy atoms in the QD-protein complex equal to 61303. Additionally, the entire QD-protein complex was solvated with explicit water molecules. The total size of the system presents an imposing challenge for computational investigation. To surmount the computational bottleneck, we have developed a multilevel approach by combining the strengths of quantum mechanics, molecular mechanics, classical molecular dynamics, and Monte Carlo techniques. The quantum dot was treated quantum mechanically, the protein was treated using molecular mechanics, and the assembly of the protein corona was performed using a combined molecular dynamics/Monte Carlo procedure. The details of the individual steps of the calculations are discussed below.

QM/MM DESCRIPTION OF THE QD-PROTEIN COMPLEX

In our QM/MM framework, only the quantum dot was treated quantum mechanically, and the protein corona surrounding the quantum dot was treated using molecular mechanics force field. The separation between the QM and the MM region is illustrated in Figure 1. One of the challenging aspects of any

Received: July 30, 2014
Published: November 17, 2014

   dx.doi.org/10.1021/ct500681m | J. Chem. Theory Comput. 2014, 10, 5224−5228

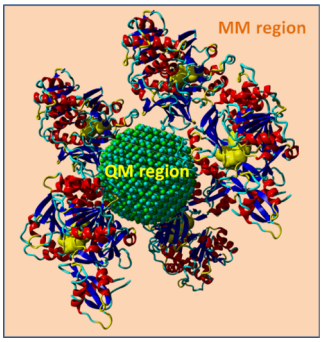

Figure 1. Separation of quantum mechanical and molecular mechanics regions for the CdSe QD (green) + firefly luciferase protein (ribbon representation) complex.

QM/MM calculation is the treatment of the QM/MM boundary, and this is a topic of ongoing research.[34,35] For systems where the QM and MM atoms are bonded chemically by covalent bonds, the QM/MM boundary can be treated using either link-atom or frozen-orbital based approaches.[34,35] However, the interaction between the protein corona and the quantum dot is known to be dominated by electrostatic interactions.[36] This nonbonding nature of the QD-protein interaction allows for a much simpler treatment of the QM/MM boundary. In the present work, the effect of protein environment was included by performing the QM calculation in the presence of the electrostatic field generated by the partial charges on the proteins. The external potential in the QM calculation was modified as shown in eq 1

$$v_{\text{ext}}^{\text{QM/MM}}(\mathbf{r}) = \sum_{k\in\text{protein}} \frac{q_k}{|\mathbf{R}_k - \mathbf{r}|} \tag{1}$$

where all terms in the above expression are in atomic units, and the magnitude and position of the partial charges on the protein are given by q_k and $\mathbf{R}_k$, respectively.

QM DESCRIPTION OF THE QUANTUM DOT

The pseudopotential approach is a computationally efficient route for performing QM calculations on large quantum dots, and we have used the empirical CdSe pseudopotential developed by Rabani et al. for this work.[37] The atomic positions were obtained from the bulk CdSe wurtzite structure, and the surface of the quantum dot was passivated with hydrogen atoms. The hydrogen atoms in the system were described using the ligand potential for passivated surface developed by Rabani et al.[37] and Wang et al.[38] The interactions with the protein corona were included in the QM calculations by adding the 1-body $v_{\text{ext}}^{\text{QM/MM}}$ term to the pseudopotential Hamiltonian. The resulting eigenvalue equation is shown in eq 2

$$\left[\frac{-\hbar^2}{2m}\nabla^2 + v_{\text{ps}}(\mathbf{r}, \mathbf{R}^{\text{dot}}) + v_{\text{ext}}^{\text{QM/MM}}(\mathbf{r}, \mathbf{R}^{\text{protein}})\right]\phi_i = \varepsilon_i\phi_i \tag{2}$$

The pseudopotential Hamiltonian was constructed using distributed Gaussian basis functions and was diagonalized to obtain the quasiparticle spectrum. The eigenvalues of the pseudupotential matrix were used for determination of the quasiparticle energy gap (E_{qp}). The quasiparticle energy gap and the optical energy gap are related to each other via the exciton binding energy, and the relationship between these three quantities is illustrated in Figure 2. The optical energy gap (E_{opt}) was obtained by first computing the exciton binding

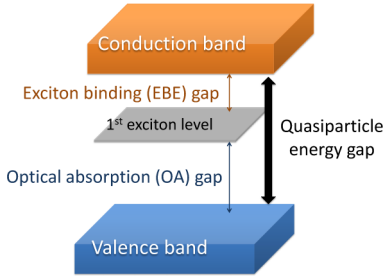

Figure 2. Relationship between optical energy gap, quasiparticle gap, and exciton binding energy.

energy ($E_{\text{bind}}^{\text{eh}}$) of the system and then subtracting the exction binding energy from the quasiparticle energy gap as shown in the following equation

$$E_{\text{opt}} = E_{\text{qp}} - E_{\text{bind}}^{\text{eh}} \tag{3}$$

The exciton binding energy was computed using the electron−hole explicitly correlated Hartree−Fock method (eh-XCHF),[39] which uses the following ansatz for the electron−hole wave function

$$\Psi_{\text{eh-XCHF}} = G\Phi_0^{\text{e}}\Phi_0^{\text{h}} \tag{4}$$

One of the key features of the eh-XCHF is that the presence of the explicitly correlated function G alleviates the need for a large CI expansion for treating electron−hole correlation.[40] In earlier studies,[41] the eh-XCHF method has been used successfully for computation of exciton binding energies in CdSe quantum dots. The electron and hole (1e-1h) basis states in the eh-XCHF wave function were obtained from the HOMO and LUMO states of the eigenspectrum of the pseudopotential Hamiltonian. The parameters used in the definition of the correlation function G were obtained from ref 41. The details of the construction of the single-particle basis functions and comparison of the eh-XCHF results with CI+pseudopotential calculations for CdSe quantum dots are presented in the Supporting Information.[42] The construction of the pseudopotential Hamiltonian requires two key pieces of information; the magnitude of the partial charges $\{q_k\}$ and their location $\{\mathbf{R}_k\}$. The determination of these two quantities are discussed below.

MM DESCRIPTION OF THE PROTEIN

The protein molecules on the surface of the CdSe quantum dot were treated classically using molecular mechanics force field. As shown in eq 1, the QM/MM interaction term is influenced by both the partial charges and the structure of the protein molecules. We have used the CHARMM36 force field for determination of the partial charges in the firefly luciferase enzyme after assigning protonation states and explicit hydrogens using PROPKA.[43] The CHARMM suite of force fields has been designed specifically for biological simulation and has been used extensively for simulating biomolecules.[44] The initial structure of the firefly luciferase enzyme was obtained from the protein data bank (PDB: 4G37)[45] and was equilibrated at 300 K by performing molecular dynamics (MD) simulations. One of the key features of the equilibration process was the use of explicit water molecules for representing the solvent environment within the MD calculations. This is an important detail,

dx.doi.org/10.1021/ct500681m | J. Chem. Theory Comput. 2014, 10, 5224−5228

because the solvated structure of the protein is generally different from its *in vacuo* structure. Equilibrating the protein in the presence of explicit water molecules allowed us to incorporate the effect of solvation and temperature in the QM/MM calculations. The equilibration runs were performed for 10 ns using the NAMD molecular dynamics package.[46] The equilibrated structure of the single protein molecule was used as the monomeric unit for the construction of the protein corona.

FORMATION OF LUCIFERASE CORONA

The two main challenges associated with protein corona formation are the QD-protein interaction and the MD simulation of the self-assembly process. Earlier studies on protein corona formation have shown that the electrostatic interaction is the dominant driving force for the corona formation.[47] For the present calculations, defining the interaction between the quantum dot and the protein is challenging because of the QM/MM separation. In principle, the QM subsystem polarizes the MM subsystem and in-turn is also polarized by the MM subsystem. Ideally, these interactions should be treated using a self-consistent procedure; however, such an approach will make the calculation impractical because of the large system size. To make the calculations feasible, we have removed the QM/MM separation and treated the entire QD-protein system classically during the corona formation. We have used the CdSe force field developed by Rabani[48] for assignment of the partial charges for Cd and Se in the quantum dot. The self-assembly of the protein corona was performed in the field of the partial charges on the quantum dot. It is very important to note that the quantum dot was treated classically *only* during formation of the protein corona and not during the optical gap calculations. Because the corona formation is complete before the QD-protein complex is electronically excited, the underlying assumption of this approach is that the set of partial charges from the CdSe force field is a good approximation to the ground state charge distribution obtained from the QM treatment of the CdSe quantum dot.

All-atom MD simulation of the self-assembly of the protein corona is challenging due to long time scales and is further exacerbated due to the presence of explicit water molecules as solvent. To make these calculations tractable, we have used a combined MD/Monte Carlo approach for this system. In the first step, the initial structure for the Monte Carlo step was obtained by arranging the protein molecules on the surface of the quantum dot. To minimize protein−protein steric interactions in the initial configuration, we have used the best-packing-on-sphere method[49] such that the center-of-mass distance between two protein molecules is maximized.[50] In the second step, the positions of Cd and Se atoms in the quantum dot were kept fixed, and the conformational degrees-of-freedom of the luciferase molecules were sampled using the Monte Carlo procedure to obtain the minimum energy structure. In the third step, the minimized structure was solvated in explicit water, and the entire system was thermally equilibrated using molecular dynamics simulation at 300 K. In the final step, the optical gap of the QD-protein complex was calculated using eq 2.

RESULTS

To facilitate the discussion of the results and analysis of the simulations, we represent the single luciferase bound complex as QD-Lu_1. The procedure described above was repeated starting with the QD-Lu_1 complex to generate QD-Lu_2. We found that up to seven luciferase molecules were able to bind with the quantum dot, and the intermediate steps of the corona formation are illustrated in Figure 3. Addition of more

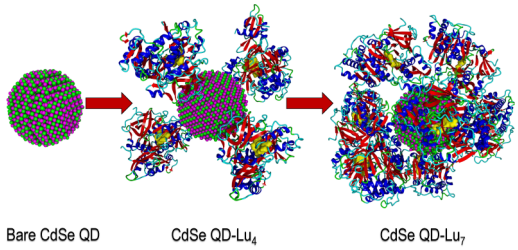

Figure 3. Progressive growth of the CdSe-luciferase protein complex.

luciferase molecules on the QD-Lu_7 complex was found to be unfavorable due to steric crowding. The atomic position of the partial charges (denoted as $\mathbf{R}^{\text{protein}}$ in eq 2) was used in the QM/MM calculations, and the optical gap E_{opt} for each of the QD-Lu_n (with n = 1, ..., 7) complexes was calculated.

The change in the optical gap of the quantum dot due to the presence of the protein is denoted as ΔE_{opt} and is defined by the following equation

$$\Delta E_{\text{opt}} = E_{\text{opt}}(\text{QD} - \text{Lu}_n) - E_{\text{opt}}(\text{QD}) \quad (5)$$

The change in the optical gap for the series of quantum dot-protein complexes during the formation of the protein corona is presented in Table 1. We find that in all cases the optical gap

Table 1. Spectral Shift Associated with Building Protein Corona around a 5 nm CdSe Quantum Dot

QD-protein	ΔE_{opt} (meV)	$\Delta\lambda_{\text{max}}$ (nm)
bare QD	0	0
QD-Lu_1	0.17	1
QD-Lu_2	4.38	2
QD-Lu_3	10.63	4
QD-Lu_4	11.02	4
QD-Lu_5	14.20	5
QD-Lu_6	22.89	7
QD-Lu_7	23.61	8

in QD-Lu_n complexes is red-shifted as compared to the bare quantum dot. The magnitude of the shift was found to increase with the increasing number of luciferase molecules. Although published experimental and computational results on CdSe-luciferase are not available, similar trends for other systems have been observed. For example, Anandampillai and co-workers have performed calculations on small CdSe-DNA clusters.[27] Their results show that the λ_{max} was red-shifted by 12 and 19 nm for dot diameters of 1.1 and 1.3 nm, respectively. Additionally, Xiong et al. have found that peptide conjugated CdTe quantum dots display a considerable redshift as compared to the bare quantum dots.[51] In the work done by Paramanik et al., a red-shift was reported for quantum dots surrounded by DNA. They concluded that the shift was mainly driven by strong electrostatic interaction between the QD and DNA.[52] Based on the reported experimental results, the shift in λ_{max} calculated in the present work is consistent with experimental findings of QD-biomolecule systems (see Figure 4).

dx.doi.org/10.1021/ct500681m | J. Chem. Theory Comput. 2014, 10, 5224−5228

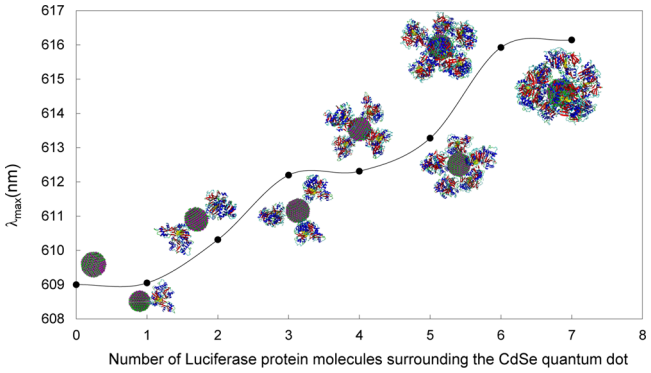

Figure 4. Shift in λ_{max} as a function of formation of protein corona around the CdSe quantum dot.

In conclusion, we have presented a multilevel strategy for calculating the optical gap of large quantum dot-protein complexes. This multilevel scheme includes techniques from quantum mechanical pseudopotential calculations, electron−hole explicitly correlated wave function, classical molecular dynamics, and the Monte Carlo method and is specifically designed to address the challenges associated with treating large quantum dot-protein complexes in aqueous medium. Although the method was applied to the specific example of the CdSe-luciferase complex, the computational strategy developed here is general and can be applied to other QD-protein complexes.

■ ASSOCIATED CONTENT

Ⓢ Supporting Information

Details of the construction of the single-particle basis functions and Figure 1. This material is available free of charge via the Internet at http://pubs.acs.org.

■ AUTHOR INFORMATION

Corresponding Authors

*E-mail: snangia@syr.edu.
*E-mail: archakra@syr.edu.

Notes

The authors declare no competing financial interest.

■ ACKNOWLEDGMENTS

We thank Professor Mathew Maye for insightful discussions. This research was funded in part by National Science Foundation grant number CHE-1349892 and by Syracuse University. This work used the Extreme Science and Engineering Discovery Environment (XSEDE), which is supported by National Science Foundation grant number ACI-1053575.

■ REFERENCES

(1) Nel, A.; Madler, L.; Velegol, D.; Xia, T.; Hoek, E.; Somasundaran, P.; Klaessig, F.; Castranova, V.; Thompson, M. Understanding biophysicochemical interactions at the nano-bio interface. *Nat. Mater.* **2009**, *8*, 543−557.

(2) Chen, Z.; Wu, D. Colloidal ZnSe quantum dot as pH probes for study of enzyme reaction kinetics by fluorescence spectroscopic technique. *Colloids Surf., A* **2012**, *414*, 174−179.

(3) Serrano, I.; Ma, Q.; Palomares, E. QD-Onion-Multicode silica nanospheres with remarkable stability as pH sensors. *J. Mater. Chem.* **2011**, *21*, 17673−17679.

(4) Medintz, I.; Stewart, M.; Trammell, S.; Susumu, K.; Delehanty, J.; Mei, B.; Melinger, J.; Blanco-Canosa, J.; Dawson, P.; Mattoussi, H. Quantum-dot/dopamine bioconjugates function as redox coupled assemblies for in vitro and intracellular pH sensing. *Nat. Mater.* **2010**, *9*, 676−684.

(5) Wang, Y.-Q.; Ye, C.; Zhu, Z.-H.; Hu, Y.-Z. Cadmium telluride quantum dots as pH-sensitive probes for tiopronin determination. *Anal. Chim. Acta* **2008**, *610*, 50−56.

(6) Liu, Y. S.; Sun, Y.; Vernier, P.; Liang, C. H.; Chong, S.; Gundersen, M. pH-sensitive photoluminescence of CdSe/ZnSe/ZnS quantum dots in human ovarian cancer cells. *J. Phys. Chem. C* **2007**, *111*, 2872−2878.

(7) Ma, Q.; Yang, F.; Ai, X.; Su, X. Dual-color quantum dot-encoded nanoprobe for DNA assays and cell imaging. *Spectrosc. Lett.* **2014**, *47*, 324−332.

(8) Wu, W.; Zhou, T.; Shen, J.; Zhou, S. Optical detection of glucose by CdS quantum dots immobilized in smart microgels. *Chem. Commun.* **2009**, 4390−4392.

(9) Nurunnabi, M.; Cho, K.; Choi, J.; Huh, K.; Lee, Y. Targeted near-IR QDs-loaded micelles for cancer therapy and imaging. *Biomaterials* **2010**, *31*, 5436−5444.

(10) Sun, X.; Huang, X.; Guo, J.; Zhu, W.; Ding, Y.; Niu, G.; Wang, A.; Kiesewetter, D.; Wang, Z.; Sun, S.; Chen, X. Self-illuminating 64 Cu-Doped CdSe/ZnS nanocrystals for in vivo tumor imaging. *J. Am. Chem. Soc.* **2014**, *136*, 1706−1709.

(11) Wu, Q.; Chu, M. Self-illuminating quantum dots for highly sensitive in vivo real-time luminescent mapping of sentinel lymph nodes. *Int. J. Nanomed.* **2012**, *7*, 3433−3443.

(12) Kumar, M.; Zhang, D.; Broyles, D.; Deo, S. A rapid, sensitive, and selective bioluminescence resonance energy transfer (BRET)-based nucleic acid sensing system. *Biosens. Bioelectron.* **2011**, *30*, 133−139.

(13) Kojima, R.; Takakura, H.; Ozawa, T.; Tada, Y.; Nagano, T.; Urano, Y. Rational design and development of near-infrared-emitting firefly luciferins available in vivo. *Angew. Chem.* **2013**, *52*, 1175−1179.

(14) Hasegawa, M.; Tsukasaki, Y.; Ohyanagi, T.; Jin, T. Bioluminescence resonance energy transfer coupled near-infrared quantum dots using GST-tagged luciferase for in vivo imaging. *Chem. Commun.* **2013**, *49*, 228−230.

(15) Hsu, C.-Y.; Chen, C.-W.; Yu, H.-P.; Lin, Y.-F.; Lai, P.-S. Bioluminescence resonance energy transfer using luciferase-immobilized quantum dots for self-illuminated photodynamic therapy. *Biomaterials* **2013**, *34*, 1204−1212.

(16) Alam, R.; Fontaine, D.; Branchini, B.; Maye, M. Designing quantum rods for optimized energy transfer with firefly luciferase enzymes. *Nano Lett.* **2012**, *12*, 3251−3256.

(17) Alam, R.; Zylstra, J.; Fontaine, D.; Branchini, B.; Maye, M. Novel multistep BRET-FRET energy transfer using nanoconjugates of firefly proteins, quantum dots, and red fluorescent proteins. *Nanoscale* **2013**, *5*, 5303−5306.

(18) Ma, N.; Marshall, A.; Rao, J. Near-infrared light emitting luciferase via biomineralization. *J. Am. Chem. Soc.* **2010**, *132*, 6884−6885.

(19) Xing, Y.; So, M.-K.; Koh, A.; Sinclair, R.; Rao, J. Improved QD-BRET conjugates for detection and imaging. *Biochem. Biophys. Res. Commun.* **2008**, *372*, 388−394.

(20) So, M.-K.; Xu, C.; Loening, A.; Gambhir, S.; Rao, J. Self-illuminating quantum dot conjugates for in vivo imaging. *Nat. Biotechnol.* **2006**, *24*, 339−343.

(21) Treuel, L.; Brandholt, S.; Maffre, P.; Wiegele, S.; Shang, L.; Nienhaus, G. Impact of protein modification on the protein corona on nanoparticles and nanoparticle-cell interactions. *ACS Nano* **2014**, *8*, 503−513.

(22) Fleischer, C.; Kumar, U.; Payne, C. Cellular binding of anionic nanoparticles is inhibited by serum proteins independent of nanoparticle composition. *Biomater. Sci.* **2013**, *1*, 975−982.

(23) Lin, C. A.; et al. Rapid transformation of protein-caged nanomaterials into microbubbles as bimodal imaging agents. *ACS Nano* **2012**, *6*, 5111−5121.

(24) Prapainop, K.; Witter, D.; Wentworth, P., Jr. A chemical approach for cell-specific targeting of nanomaterials: Small-molecule-

initiated misfolding of nanoparticle corona proteins. *J. Am. Chem. Soc.* **2012**, *134*, 4100−4103.
(25) Nangia, S.; Sureshkumar, R. Effects of Nanoparticle Charge and Shape Anisotropy on Translocation through Cell Membranes. *Langmuir* **2012**, *28*, 17666−17671.
(26) Pease, L.; Feldblyum, J.; Depaoli Lacaerda, S.; Liu, Y.; Hight Walker, A.; Anumolu, R.; Yim, P.; Clarke, M.; Kang, H.; Hwang, J. Structural analysis of soft multicomponent nanoparticle clusters. *ACS Nano* **2010**, *4*, 6982−6988.
(27) Anandampillai, S.; Zhang, X.; Sharma, P.; Lynch, G. C.; Franchek, M.; Larin, K. Quantum dot-DNA interaction: Computational issues and preliminary insights on use of quantum dots as biosensors. *Computer Methods Appl. Mechanics Eng.* **2008**, *197*, 3378−3385.
(28) Kim, H.-S.; Jang, S.-W.; Chung, S.-Y.; Lee, S.; Lee, Y.; Kim, B.; Liu, C.; Neuhauser, D. Effects of Bioconjugation on the Structures and Electronic Spectra of CdSe: Density Functional Theory Study of CdSe-Adenine Complexes. *J. Phys. Chem. B* **2010**, *114*, 471−479.
(29) Kilina, S.; Velizhanin, K. A.; Ivanov, S.; Prezhdo, O. V.; Tretiak, S. Surface Ligands Increase Photoexcitation Relaxation Rates in CdSe Quantum Dots. *ACS Nano* **2012**, *6*, 6515−6524.
(30) Abuelela, A. M.; Mohamed, T. A.; Prezhdo, O. V. DFT Simulation and Vibrational Analysis of the IR and Raman Spectra of a CdSe Quantum Dot Capped by Methylamine and Trimethylphosphine Oxide Ligands. *J. Phys. Chem. C* **2012**, *116*, 14674−14681.
(31) Fischer, S. A.; Crotty, A. M.; Kilina, S. V.; Ivanov, S. A.; Tretiak, S. Passivating ligand and solvent contributions to the electronic properties of semiconductor nanocrystals. *Nanoscale* **2012**, *4*, 904−914.
(32) Albert, V. V.; Ivanov, S. A.; Tretiak, S.; Kilina, S. V. Electronic Structure of Ligated CdSe Clusters: Dependence on DFT Methodology. *J. Phys. Chem. C* **2011**, *115*, 15793−15800.
(33) Kilina, S.; Ivanov, S.; Tretiak, S. Effect of Surface Ligands on Optical and Electronic Spectra of Semiconductor Nanoclusters. *J. Am. Chem. Soc.* **2009**, *131*, 7717−7726.
(34) Senn, H. M.; Thiel, W. QM/MM Methods for Biomolecular Systems. *Angew. Chem.* **2009**, *48*, 1198−1229.
(35) Lin, H.; Truhlar, D. QM/MM: what have we learned, where are we, and where do we go from here? *Theor. Chem. Acc.* **2007**, *117*, 185−199.
(36) Mattoussi, H.; Mauro, J. M.; Goldman, E. R.; Anderson, G. P.; Sundar, V. C.; Mikulec, F. V.; Bawendi, M. G. Self-Assembly of CdSe-ZnS Quantum Dot Bioconjugates Using an Engineered Recombinant Protein. *J. Am. Chem. Soc.* **2000**, *122*, 12142−12150.
(37) Rabani, E.; Hetenyi, B.; Berne, B. J.; Brus, L. E. Electronic properties of CdSe nanocrystals in the absence and presence of a dielectric medium. *J. Chem. Phys.* **1999**, *110*, 5355−5369.
(38) Wang, L.-W.; Zunger, A. Pseudopotential calculations of nanoscale CdSe quantum dots. *Phys. Rev. B* **1996**, *53*, 9579.
(39) Elward, J. M.; Thallinger, B.; Chakraborty, A. Calculation of electron-hole recombination probability using explicitly correlated Hartree-Fock method. *J. Chem. Phys.* **2012**, *136*, 124105.
(40) Elward, J. M.; Hoja, J.; Chakraborty, A. Variational solution of the congruently transformed Hamiltonian for many-electron systems using a full-configuration-interaction calculation. *Phys. Rev. A* **2012**, *86*, 062504.
(41) Elward, J. M.; Chakraborty, A. Effect of Dot Size on Exciton Binding Energy and Electron-Hole Recombination Probability in CdSe Quantum Dots. *J. Chem. Theory Comput.* **2013**, *9*, 4351−4359.
(42) Details of the construction of the single-particle basis functions are presented in the Supporting Information.
(43) Olsson, M. H. M.; Sondergaard, C. R.; Rostkowski, M.; Jensen, J. H. PROPKA3: Consistent Treatment of Internal and Surface Residues in Empirical pKa Predictions. *J. Chem. Theory Comput.* **2011**, *7*, 525−537.
(44) Best, R. B.; Zhu, X.; Shim, J.; Lopes, P. E. M.; Mittal, J.; Feig, M.; MacKerell, A. D. Optimization of the Additive CHARMM All-Atom Protein Force Field Targeting Improved Sampling of the Backbone ϕ, ψ and Side-Chain x_1 and x_2 Dihedral Angles. *J. Chem. Theory Comput.* **2012**, *8*, 3257−3273.
(45) Sundlov, J. A.; Fontaine, D. M.; Southworth, T. L.; Branchini, B. R.; Gulick, A. M. Crystal Structure of Firefly Luciferase in a Second Catalytic Conformation Supports a Domain Alternation Mechanism. *Biochemistry* **2012**, *51*, 6493−6495.
(46) Phillips, J. C.; Braun, R.; Wang, W.; Gumbart, J.; Tajkhorshid, E.; Villa, E.; Chipot, C.; Skeel, R. D.; KalÃl', L.; Schulten, K. Scalable molecular dynamics with NAMD. *J. Comput. Chem.* **2005**, *26*, 1781−1802.
(47) Casals, E.; Pfaller, T.; Duschl, A.; Oostingh, G. J.; Puntes, V. Time Evolution of the Nanoparticle Protein Corona. *ACS Nano* **2010**, *4*, 3623−3632.
(48) Rabani, E. Structure and electrostatic properties of passivated CdSe nanocrystals. *J. Chem. Phys.* **2001**, *115*, 1493−1497.
(49) Saff, E. B.; Kuijlaars, A. B. J. Distributing many points on a sphere. *Mathematical Intelligencer* **1997**, *19*, 5−11.
(50) King, N. P.; Bale, J. B.; Sheffler, W.; McNamara, D. E.; Gonen, S.; Gonen, T.; Yeates, T. O.; Baker, D. Accurate design of co-assembling multi-component protein nanomaterials. *Nature* **2014**, *510*, 103−108.
(51) Xiong, R.; Li, Z.; Mi, L.; Wang, P.-N.; Chen, J.-Y.; Wang, L.; Yang, W.-L. Study on the Intracellular Fate of Tat Peptide-Conjugated Quantum Dots by Spectroscopic Investigation. *J. Fluoresc.* **2010**, *20*, 551−556.
(52) Paramanik, B.; Bhattacharyya, S.; Patra, A. Steady state and time resolved spectroscopic study of QD-DNA interaction. *J. Lumin.* **2013**, *134*, 401−407.